Biosensors and Bioelectronics 143 (2019) 111597

Contents lists available at ScienceDirect

Biosensors and Bioelectronics

journal homepage: www.elsevier.com/locate/bios

A digital microfluidic diluter-based microalgal motion biosensor for marine pollution monitoring

Shuang Han[a,f,1], Qian Zhang[a,f,1], Xingcai Zhang[b,1], Xianming Liu[d,f], Ling Lu[c,f], Junfeng Wei[a,f], Yuancheng Li[e,**], Yunhua Wang[c,f,***], Guoxia Zheng[a,f,*]

[a] Environmental and Chemical Engineering Institute, Dalian University, Dalian, 116622, China
[b] John A. Paulson School of Engineering and Applied Sciences, Harvard University, Cambridge, MA, 02138, United States
[c] Dalian Institute of Chemical Physics, Chinese Academy of Sciences, Dalian, 116023, China
[d] Medical School, Dalian University, Dalian, 116622, China
[e] The First Affiliated Hospital of Dalian Medical University, Dalian, 116001, China
[f] Environmental Micro Total Analysis Lab, Dalian University, Dalian, 116622, China

ARTICLE INFO

Keywords:
Algae biosensor
Motility signal
Digital microfluidics
Marine monitoring
Feedback control
Cross-split

ABSTRACT

Marine pollution and monitoring have received more and more concern in recent years. Herein, a fully automatic whole-algae biosensor was designed for low-cost and fast detection of toxic contaminants in seawater. It consists of a digital microfluidic (DMF) diluter chip, an actuation element, a detector element, and a microalgae bioreporter. A feedback-control protocol based on charging-time compensation was introduced. It ensures precise actuation of the droplet with diverse salty concentrations and contents in the marine environment. The two-mixer cross-split dilution engine increases the accuracy of droplet dispensing and concentration diluting. By selecting motility of *P. subcordiformis* as the sensor signal, the developed biosensor showed good sensitivity and robustness for a wide range of salinity (10–37‰), temperature (0–25 °C), light levels (0–325 μmol photons m^{-2} s^{-1}), and cell density factor (1.0–4.0). The biosensor responses were examined in the presence of copper, lead, phenol, and nonylphenol (NP). In all cases, toxic responses (i.e. dose-related inhibition of algal motion) were detected with the detection limits of 0.65 μmol.L^{-1}, 1.90 μmol.L^{-1}, 2.85 mmol.L^{-1}, and 5.22 μmol.L^{-1} respectively. These results were obtained in a much shorter time (2 h for our biosensor vs. 24 h-10 d for growth inhibition test) and the data are consistent with previous classical studies. We thus developed a simple, rapid, and adaptable system for marine routine monitoring and early-warning detection for lab and on-site applications.

1. Introduction

Over the last few decades, the marine environment has been increasingly exposed to anthropogenic pollutants, which became a big concern in ocean governance, including effective monitoring and regulation. The exploration of convenient methods or parameters for assessing pollutants and their toxicity has become a major goal in modern marine environmental monitoring research. Biomarker assays have been widely used to evaluate the bioavailability of pollutants and their potential risks on marine ecological environments (Hook et al., 2014). Biosensors based on biomarker assays have shown great potential in the development of portable, fast, and economical analysis methods (Kissinger, 2005; Amine et al., 2006).

Microalgae have been widely used as relevant biological recognition element in the fabrication of biosensors, owing to their ecological significance, ubiquity, short life cycles, easiness of culture, and high sensitivities to many pollutants (Satoh et al., 2005; Pham et al., 2010; Turemis et al., 2018). In the alga bioassay, microalgae responded to the target compound with a detectable signal in a dose-effective manner. Growth rate, fluorescence induction, photosynthetic function, and metabolism (esterase activity) are the most popular endpoints studied. Growth inhibition, the most used trait in bioassays for environmental management of chemical discharges, generally need 48–96 h of chronic exposure which is not suitable for emergency monitoring. The durations

* Corresponding author. Environmental and Chemical Engineering Institute, Dalian University, Dalian, 116622, China.
** Corresponding author. The First Affiliated Hospital of Dalian Medical University, Dalian, 116001, China.
*** Corresponding author. Medical School, Dalian University, Dalian, 116622, China.
E-mail addresses: yuancheng1999@163.com (Y. Li), yunhua1977@126.com (Y. Wang), guoxiazheng2685@163.com (G. Zheng).
[1] These authors contribute equally.

https://doi.org/10.1016/j.bios.2019.111597
Received 29 June 2019; Received in revised form 11 August 2019; Accepted 13 August 2019
Available online 14 August 2019
0956-5663/

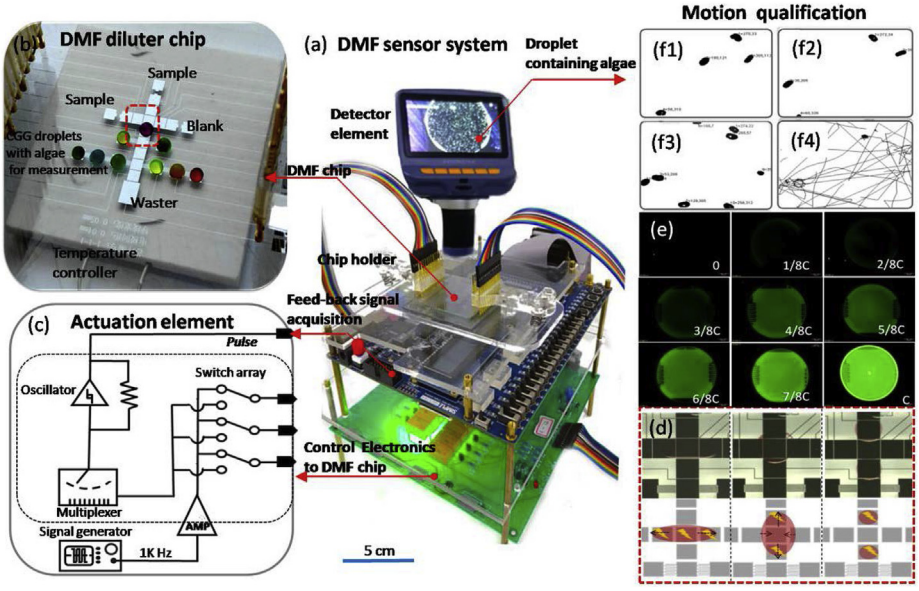

Fig. 1. Proposed control-engaged DMF sensor technology. (a) The sensor system consists of a DMF diluter chip, an actuation element, and a detector element. The actuation element include two units: one for the generation and amplification of alternating current (AC) square wave signal used for actuation; the other one is a field-programmable gate array (FPGA)-based controller unit for multiple operations including sequential and programmable droplet transportation, actuation mode (operation unit) and position sensor mode switching, feedback-based position calculation, data integrating, and actuation signal outputting. (b) Three-dimensional schematic of DMF chip. A temperature controller was integrated into the chip holder. (c) Overview schematic of the droplet control system. (d) Droplet cross-split way used in this study (Views from the red dashed box in (b)). Voltage was applied on electrodes, as marked with a yellow sign. Accordingly, the droplet (red) will be stretched horizontally and subsequently split into vertical phases. (e) Dilution performance validation. As the fluorescence intensity of Rh-123 was proportional to its concentration, the intensities of Rh-123 at nine droplets generated by DMF diluter were imaged by an inverted fluorescence microscope. (f) Alga motion qualification by Image-J with the represented movement tracking shown in the first frame (f1), the second frame, and (f2) the third frame (f3). Paths for microalgae present throughout all frames in tests were shown in (f4). Each black path corresponds to a single trajectory. (For interpretation of the references to colour in this figure legend, the reader is referred to the Web version of this article.)

of assays based on other physiological traits were relatively short (2–4 h). However, those alga sensors usually need appropriate sampling, several dilutions, pre-immobilization of microalgae, poison stressing, and physiological traits detection. Those tests are off-line, laborious, and not easy to handle (Pea-Vázquez et al., 2009). Beyond the above-mentioned physiological traits, the algal motion is a reliable indicator. Most microalgae in the marine euphotic zone are motile (Donaghay and Osborn, 1997). They can swim in complex trajectories (Chengala et al., 2013) that allow them to explore and interact with the surrounding environment. Spatial gradients of chemical stimuli may alter microorganism swimming behavior and cause chemotaxis (Fenchel, 2002) towards a range of important ecological phenomena including predator-prey interactions, patchiness of nutrients, avoidance or sex (Seymour et al., 2010). Thus, the microalgal motion could be used as a sensitive sensor to marine chemical signals and a linkage between biochemical processes on the sub-cell level and ecological consequence on the ecosystem level. Several parameters measured by computer-assisted movement tracking, including motility determination parameters, velocity parameters, and motion manner, have been used to characterize microalgal locomotion and to demonstrate the toxic effect of hazardous chemicals (Liu et al., 2011; Han et al., 2019). In these assays, the whole cell of mobile algae worked as a reporter and could be traced in the light field free from high-power lasers or LEDs. They may provide simpler alternatives to fluorescence-based algal assays (e.g. photosynthetic activity and esterase activity assays) for developing biosensor systems. However, few studies have focused on such type of biosensors, due to the absence of user-friendly operating tools, especially those integrating fluid units for mobile algae that can avoid cell entrapment and maintain cell motility.

To enhance the efficiency of biosensors, microfluidics technology is gaining importance in recent years (Zhu et al., 2017; Shi.et al., 2018). Microfluidic systems can offer cost- and time-efficient alternatives by integrating multiple processes on a single platform and providing high-precision and high-efficiency cell/reagent handling capabilities. This is especially true for digital microfluidics (DMF) which manipulates discrete droplets by ElectroWetting On Dielectric (EWOD) (Jebrail et al., 2012). It has many advantages that are absent from channel-based microfluidics. It is fully programmable, reconfigurable, hardware (e.g. pumps, valves) liberal, and extremely energy efficient (Jebrail et al., 2012; Zhang et al., 2019). Especially, high-throughput dilutions can be simply and robotically achieved by multiple mixing-splitting operations (Roy et al., 2014; Wang et al., 2017). This brings particular convenience for laboratory routine analysis or on-site marine monitoring.

In this proof-of-concept study, we established a fully automatic DMF diluter-based algal biosensor using microalgal motility measurement for marine monitoring. To upgrade the system accuracy and stability, a feedback control loop was included into DMF control module. All droplets were addressed by the droplet-derived real-time capacitance scanning (Murran and Najjaran, 2012). Besides, an innovative "cross-split" two-mixer dilution engine was used to generate droplets containing polluted seawaters with concentration gradients. We assessed the DMF properties by measurements of arriving completion, splitting volumetric error, and fluorescence intensity of target droplets. Microalgal actuating compatibility and device performance were evaluated using four dominant sea species of motile microalgae (*Platymonas subcordiformis*, *Platymonas helgolandica var. tsingtaoensis, Isochrysis galbana,* and *Isochrysis zhanjiangensis* sp.*nov.*) in Chinese coastal waters (Table S1). Besides hardware building, a number of methodological and operational conditions (i.e. alga strains, saline condition, irradiance, temperature, cell density, and measurement parameters including Percent motile cells of total cells (MOT %), Curvilinear velocity (VCL), Average path velocity (VAP), and Straight-line velocity (VSL) (Table S3) were selected and standardized to improve the stability and adaptability of the microalgae biosensor. Finally, selected microalgal species and measurement parameter, as well as essential operation conditions, were integrated into the DMF device, including a DMF diluter chip together with actuation units and detector elements. The sensor signals of alga motility were tested in marine water samples spiked with typical anthropogenic contaminants (heavy metals and phenols). The results were compared with conventional algal bioassays.

2. Results and discussions

The biosensor device shown in Fig. 1 was designed to generate serial diluted polluted seawater droplets containing algae and integrated with microalgal motion measurements (MOT%, VCL, VAP, and VSL). The analyzing procedure is summarized in Fig. S3. Briefly, polluted seawaters and buffer with algal cell suspension were loaded (Fig. S3a).

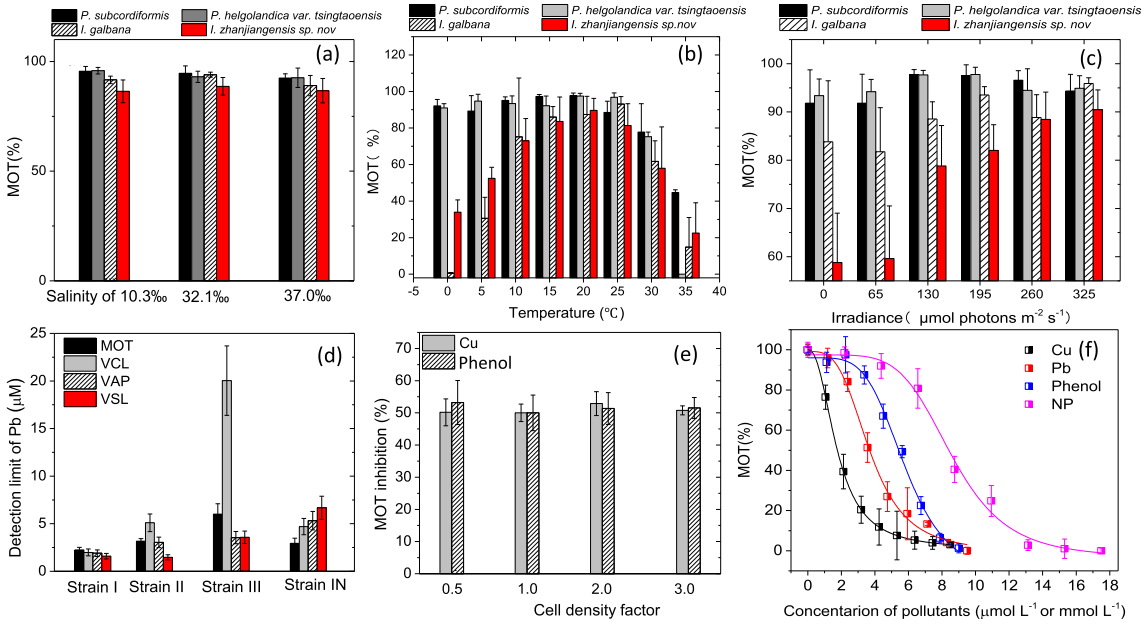

Fig. 2. Influences of (a) Salinity (b) Temperature, and (c) Illuminance on characteristic parameters of MOT% of the four test algae strains. (d) Represented test sensitivity of different algae species (Strain I: *P. subcordiformis,* Strain II: *P. helgolandica var. tsingtaoensis*, Strain III: *I. galbana* and Strain IV: *I. zhanjiangensis* sp.*nov.*) to Pb (e) Influences of different initial cell density (*P. subcordiformis*) on toxicity test evaluated by use of MOT inhibitions (%). (f) Dose-response curves for typical marine pollutants (Cu, Pb, and NP based on the μmol L^{-1} range and phenol based on mmol L^{-1} range) depending on bioreporter's (*P.subcordiformis*) MOT% measurement.

Multiple mix-split cycles were applied to generate arrays of droplets containing serials concentrations (C) of pollutant (0, 1/8C, 2/8C, 3/8C, 4/8C, 5/8C, 6/8C, 7/8C, and C), respectively, for screening (Fig. S3b). The motion measurements were collected after a brief incubation (Fig. S3c). Several design iterations were required to develop such kind of devices. The two main challenges were the accurate actuation of seawater droplets and reliable concentration gradient generation.

During droplet movement from one electrode to its neighbor, a continuous state of actuation occurs. It was found that the EWOD-force-induced displacements of saline (10‰–37‰) droplets versus the actuation time exhibit distinct slope profiles of each other (Fig. S4a). The actual droplet positions (measured from the top-view images taken by camera) deviate from the theoretical value (computed using equation (2) in the supplementary information) depending on salinity variation (Fig. S4b). These different behaviors in the movement of actual seawater samples, confirmed by our experiments, serve as the core rationale for setting up a feedback control protocol. In this work, the charging time was chosen as the compensation parameter that can be automatically adjusted by the control-coordinating program. When a droplet decays, the droplet position can be sensed by real-time capacitance scanning and additional charging time will be applied repeatedly until the droplet reached the destination. To find an optimum threshold resistance (R_{thresh}), six trials from 0.55 to 0.8 were tested. In a 5-steps movement with 10 trials, 100% completion can be achieved when R_{thresh} ranges from 0.7 to 0.8. The robustness of the results for R_{thresh} from 0.7 to 0.8 indicates that the proposed feedback system can effectively manipulate seawater droplet without extra calibration. As listed in Table S3, the percent (%) completion of different seawaters without extra calibration at R_{thresh} = 0.75 were studied to validate the feedback-enhanced droplet movement. It was found that the seawaters with salinities of 10.3‰, 32.1‰, and 37.0‰, fitting the wide saline range from the estuary, coastal area, and open sea, can be transported with 100% completion.

In response to an accurate concentration gradient generation, the two-mixer dilution engine needs minimum mix-split steps. As described in the dilution tree, up to three mix-split steps were used (Fig. S2). The reduced mix-split steps minimized total error. As shown in Fig. 1d and supplementary movie file, an innovative “cross-split” way was used here for a more reliable droplet dispensing. It can avoid abnormal dividing which is common in a traditional stretching-split way (Table S5). The average volumetric errors (cross-split) of DI water and seawaters with salinities of 10.3‰, 32.1‰, and 37.0‰ were all lower than 1.5%. Their maximum total errors were about 2% (Table S5). To further verify the proposed dilution process, a series of parallel dilution experiments were performed. Fig. 1e shows the droplets generated with diluted concentration ratios of 0, 1/8, 2/8, 3/8, 4/8, 5/8, 6/8, 7/8, and 8/8. The intensities of Rh-123 in nine droplets were quantified and compared with the theoretical data. There was a good coherence (correlation coefficient = 0.995) between the experimental and theoretical data (Fig. S5).

The effect of DMF actuation voltage on the cell vitality was evaluated by measuring the motion of four marine motile microalgae. The actuated and non-actuated algae were compared immediately after actuation and after 24 h incubation in a humidified incubator. There were no significant differences between actuated and non-actuated algae at 0 h and 24 h for all tested strains ($p > 0.05$, Fig. S6). These results suggested that DMF actuation does not significantly alter cell vitality. Furthermore, most algae (> 90%) were motile through 24 h culture on DMF and there was no significant difference in swimming velocity at 0 h and 24 h time points ($p > 0.05$). The maintaining of cell mobility over this time period indicated the compatibility of the device, which was important for toxicity test control.

To improve the response of the biosensor, the microalgae strain, characteristic parameters, and operating conditions were optimized. Under different operating conditions, the characteristic parameters MOT%, VCL, VAP, and VSL were analyzed. The effects of sample salinity were evaluated at saline values ranging from 10‰ to 37‰. The results showed that signals were generally the same for the four microalgae tested ($p < 0.05$, Fig. S7a), providing that the developed biosensor was robust to wide saline concentrations. The effects of temperatures (0–35 °C) and irradiance levels (0–325 μmol photons m^{-2} s^{-1}) were measured, too (Figs. S7b and c). Temperature and irradiance exerted strong influences on the swimming speed (VCL, VAP, and VSL) of the four marine microalgae, with the optimal conditions found at

about 20 °C and 195–260 μmol photons m^{-2} s^{-1}. However, MOT% of *Platymonas* showed a high tolerance to a wide range of temperature (0–25 °C) and light levels (0–325 μmol photons m^{-2} s^{-1}). Especially, most *Platymonas* (> 90%) were motile at extremely cold and dark surroundings (0 °C and 0 μmol photons m^{-2} s^{-1}) (Fig. 2). These results suggested that temperature and irradiance need not to be strictly controlled when using *Platymonas* and characteristic parameter of MOT% to perform biosensing.

The responses of algal strains on typical anthropogenic contaminants (heavy metals and phenols) were measured. Detection limits calculated from fitted sigmoid equations of the Hill model were summarized in Figs. S8a–d. Obviously, microalgal motion was inhibited in a different manner, depending on the species of microalga. *P. subcordiformis* motion signal appeared to be the most sensitive to the tested pollutants among the four marine microalgae (Fig. 2d). When taking test sensitivity and operation adaptability into comprehensive consideration, *P. subcordiformis* would be the optimal test strain and MOT% can be a good detection parameter for biosensing.

Furthermore, the effects of cell density on the biosensing response to copper and phenol were evaluated for *P. subcordiformis*. The results showed that signals were generally consistent for the four cell density levels ($p < 0.05$) (Fig. 2e), implying that cellular density does not need to be carefully controlled for biosensor development using algal motion measurement.

The responses of the improved biosensor were tested using natural marine water samples (Table S2) spiked with typical anthropogenic contaminants (heavy metals and phenols). The variation of MOT% from the selected bioreporter i.e. *P. subcordiformis* (in a logarithmic phase $\sim 4 \times 10^5$ cells ml^{-1}) at 20 ± 1 °C, 32.1‰ salinity and 200 μmol photons m^{-2} s^{-1} was monitored. The observed MOT% depended on the concentration of pollutants (Fig. 2f). The calculated detection limits and EC_{50} values for these pollutants were listed in Table 1. Several methods using microalgae as bioreporter for environmental monitoring and risk assessment have been listed in Table S6. Compared with classical algae-based toxicity screening, our system needs less sensing time (2 h for our biosensor vs. 24 h-10 d for growth inhibition method), while showing similar sensitivity within detection limits and EC_{50} values (in micromole range for heavy metals and NP; millimole range for phenol). Moreover, this proposed system was fully automatic, with the lowest level of manual intervention (i.e. no sample dilution and algae pre-immobilization steps compared to traditional algae-sensors). With the specific DMF diluter design and applying *P. subcordiformis* as bioreporter, it gives the possibility to operate continuously and rapidly for toxicity detection in the lab and on site.

For validation purposes, the Cu and phenol samples were analyzed by anodic stripping voltammetry (ASV) and high-performance liquid chromatography (HPLC), respectively, in parallel with biosensor analyses. Four independent measurements were performed. The biosensor analysis reported a Cu concentration of 1.51 ± 0.5 μmol L^{-1} and a phenol concentration of 10.2 ± 1.5 mmol L^{-1}. The obtained concentration values of Cu (ASV) and phenol (HPLC) were 1.45 ± 0.5 μmol L^{-1} and 10.7 ± 1.3 mmol L^{-1}, respectively. Values for both methods were statistically compared and no significant difference was found ($p > 0.05$). Therefore, the microalgal biosensor was accurate for toxicant determinations.

The reproducibility and repeatability of biosensor were evaluated by MOT inhibition measurements. Three droplets of 1.67 μmol L^{-1} (EC_{50}) Cu or 6.07 mmol L^{-1} (EC_{50}) phenol containing bioreporters (in a logarithmic phase $\sim 2 \times 10^5$ to $\sim 4 \times 10^5$ cells ml^{-1}) were prepared independently at different days with randomized experimental condition (salinity of 10.3‰–37.0‰, temperature of 18–21 ± 1 °C, light condition of ~80–~100 μmol photons m^{-2} s^{-1}). The RSD for each EC_{50} values Cu and phenol measurement (n = 6) were 2.1% and 1.5%, respectively, revealing the good repeatability and operation robustness of the proposed system (Table S7). Meanwhile, the consistent EC_{50} values measured at different salinity backgrounds (Table S2) illustrated that the coexisting ions (such as mercury, cadmium) and substances (phenol and NP) in seawater will not interfere with biosensing actively. It implied that all the coexisting ions and substances in the obtained seawater sample were under their detection limits. If the DMF diluter-based biosensor was used to monitor highly contaminated sea water, it will evaluate comprehensive effects of mixtures of various chemical other than single toxicity selectively.

Table 1
DMF biosensor response to different typical anthropogenic contaminants.

Pollutant	Detection limit (MOT %)	EC_{50} (MOT %)	Dynamic range
Cu (μmol L^{-1})	0.65 ± 0.04	1.67 ± 0.09	0.95–3.22
Pb (μmol L^{-1})	1.90 ± 0.24	3.83 ± 0.51	2.42–5.54
Phenol (mmol L^{-1})	2.85 ± 0.28	6.07 ± 0.79	3.87–7.01
NP (μmol L^{-1})	5.22 ± 1.62	8.60 ± 2.29	6.34–10.87

3. Conclusions

An integrated biosensor system was developed by combining miniaturization/automation potential of DMF and broad-spectra sensitivity/robustness of algae motion signal. A feedback control loop was included to overcome the potential risk of driven failure, induced by diversity contents in seawaters. Meanwhile, two-mixer dilution engine with minimum mix-split steps in a cross-split way was used to ensure precise dispensing of droplets.

The influence of physical conditions (salinity, temperature, and luminance) on sensor responses and the influence of algae strains and cell density on sensor sensitivity were evaluated. As a consequence, the *P. subcordiformis* was the most sensitive bioreporter with high robustness to salinity, temperature, illuminance, and cell density. It was encapsulated in our newly developed biosensor for the detection of marine pollutants by motility analysis. The detection limits of this biosensor were in the μmol l^{-1} range for toxic metals and NP and in the mmol l^{-1} range for phenol. These results were consistent with previous classical toxicity screening data, with a much shorter sensing time (2 h for our biosensor vs. 24 h-10 d for growth inhibition test). The high accuracy, repeatability, and robustness were also well demonstrated. This new biosensor showed huge potential in marine routine monitoring and early-warning detection in the lab or on-site.

CRediT authorship contribution statement

Shuang Han: Investigation. **Qian Zhang:** Investigation. **Xingcai Zhang:** Investigation, Writing - review & editing. **Xianming Liu:** Software. **Ling Lu:** Data curation. **Junfeng Wei:** Formal analysis. **Yuancheng Li:** Methodology, Writing - review & editing. **Yunhua Wang:** Conceptualization, Writing - review & editing. **Guoxia Zheng:** Conceptualization, Methodology, Writing - original draft.

Declaration of competing interest

The authors declare that they have no known competing financial interests or personal relationships that could have appeared to influence the work reported in this paper.

The authors declare the following financial interests/personal relationships which may be considered as potential competing interests:

Acknowledgments

This work was supported by the National Natural Science Foundation of China (No. 41476085, No. 81471807) and the Scientific Research Project of Liaoning Education Department (LJQ 2015005).

Appendix A. Supplementary data

Supplementary data to this article can be found online at https://doi.org/10.1016/j.bios.2019.111597.

References

Amine, A., Mohammadi, H., Bourais, I., Palleschi, G., 2006. Biosens. Bioelectron. 21, 1405–1423.

Chengala, A., Hondzo, M., Sheng, J., 2013. Phys. Rev. E 87 (5–1), 1–16.

Donaghay, P.L., Osborn, T.R., 1997. Limnol. Oceanogr. 42, 1283–1296.

Fenchel, T., 2002. Science 296, 1068–1071.

Han, B.X., Zheng, G.X., Wei, J.F., Yang, Y.S., Lu, L., Zhang, Q., Wang, Y.H., 2019. Bioproc. Biosyst. Eng. 1-13.

Hook, S.E., Gallagher, E.P., Batley, G.E., 2014. Integr. Environment. Asses. 10, 327–341.

Jebrail, M.J., Bartsch, M.S., Patel, K.D., 2012. Lab Chip 12, 2452–2463.

Kissinger, P.T., 2005. Biosens. Bioelectron. 20, 2512–251620.

Liu, G.X., Chai, X.L., Shao, Y.Q., Hu, L.H., Xie, Q., Wu, H.X., 2011. J. Environ. Sci. China 23 (2), 330–335.

Murran, M.A., Najjaran, H., 2012. Lab Chip 12, 2053–2059.

Pea-Vázquez, E., Maneiro, E., Pérez-Conde, C., Moreno-Bondi, M.C., Costas, E., 2009. Biosens. Bioelectron. 24, 3538–3543.

Pham, T.P.T., Cho, C.-W., Yun, Y.-S., 2010. Algal biosensor-based measurement system for rapid toxicity detection. In: Milind, K.S. (Ed.), Advances in Measurement Systems. E-Publishing Inc., London, pp. 274–288.

Roy, S., Bhattacharya, B.B., Ghoshal, S., Chakrabarty, K., 2014. J. L. P. Electron, vol. 10. pp. 506–518 13.

Satoh, A., Vudikaria, L.Q., Kurano, N., Miyachi, S., 2005. Environ. Int. 31, 713–722.

Seymour, J.R., Simó, R., Ahmed, T., Stocker, R., 2010. Science 329, 329–342.

Shi, Y., Liu, H.L., Zhu, X.Q., Zhu, J.M., Zuo, Y.F., Yang, Y., Jiang, F.H., Sun, C.J., Zhao, W.H., Han, X.T., 2018. Lab Chip 18, 2994–3002.

Turemis, M., Siletti, S., Pezzotti, G., Sanchís, J., Farré, M., Giardi, M.T., Moro, L., 2018. Sens. Actuators B Chem. 270, 424–432.

Wang, Y.B., Huang, J.H., Lee, M., Huang, S., C.Y, Huang, C.S., Yamashita, I., Tu, Y.Y., Hsu, W., 2017. Microsyst. Technol. 23, 3645–3651.

Zhang, Q., Zhang, X., Zhang, X., Jiang, L., Yin, J., Zhang, P., Han, S., Wang, Y., Zheng, G., 2019. Mar. Pollut. Bull. 144, 20–27.

Zhu, J.M., Shi, Y.X., Zhu, Q., Yang, Y., Jiang, F.H., Sun, C.J., Zhao, W.H., Han, X.T., 2017. Lab Chip 17, 4025–4030.